Mediterranean Marine Science

Vol 18, No 2 (2017)

A multiplatform investigation of Istrian Front dynamics (north Adriatic Sea) in winter 2015

Z. KOKKINI, R. GERIN, P.M. POULAIN, E. MAURI, Z. PASARIĆ, I. JANEKOVIĆ, M. PASARIĆ, H. MIHANOVIĆ, I. VILIBIĆ

doi: 10.12681/mms.1895

Research Article

Mediterranean Marine Science
Indexed in WoS (Web of Science, ISI Thomson) and SCOPUS
The journal is available on line at http://www.medit-mar-sc.net
DOI: http://dx.doi.org/10.12681/mms.1895

A multiplatform investigation of Istrian Front dynamics (north Adriatic Sea) in winter 2015

Z. KOKKINI[1], R. GERIN[1], P. M. POULAIN[1], E. MAURI[1], Z. PASARIĆ[2], I. JANEKOVIĆ[3, 4], M. PASARIĆ[2], H. MIHANOVIĆ[5] and I. VILIBIĆ [5]

[1] Istituto Nazionale di Oceanografia e di Geofisica Sperimentale – OGS, Trieste, Italy
[2] Department of Geophysics, Faculty of Science, University of Zagreb, Zagreb, Croatia
[3] Rudjer Boskovic Institute, Division for Marine and Environmental Research, Zagreb, Croatia
[4] School of Civil, Environmental, and Mining Engineering & UWA Oceans Institute, The University of Western Australia, Perth, Australia
[5] Institute of Oceanography and Fisheries, Croatia, Split, Physical Oceanography Laboratory

Corresponding author: zkokkini@inogs.it

Handling Editor: Takvor Soukissian

Received: 2 September 2016; Accepted: 22 May 2017; Published on line: 31 July 2017

Abstract

In the northeastern Adriatic Sea, southwest of the Istrian Peninsula, a persistent thermohaline front is formed, which is herein called the Istrian Front (IF). A Slocum glider was operated across the IF near the entrance to Kvarner Bay between 24 and 27 February 2015. Three Acoustic Doppler Current Profilers (ADCPs) were also deployed at the entrance of Kvarner Bay during the same period. The glider crossed the IF twice, during which the IF was characterized by its fast response to local wind conditions, and strong salinity, temperature and density gradients were detected. During the first crossing, a strong northeasterly Bora wind was blowing. This resulted in a very sharp and strong thermohaline front, which extended vertically throughout the entire water column between saltier and warmer water to the south, and fresher and colder water to the north. Across the front, the SST changed ~ 1.2° C within a distance of 2.4 km. In contrast, during the second crossing, which was approximately 2 days later and under weaker wind conditions, the IF appeared to be much smoother, inclined and wider, and the SST changed ~ 1.2° C within a distance of 8 km. A strong density gradient was also reported, which was coincident with the thermohaline IF. From previous observations, primarily experiments in 2003, the IF was known only as a thermohaline front compensated in density. In the winter of 2015, the density front was strong and well defined, demonstrating a density difference of approximately 0.36 kg/m^3 within a distance of 2.4 km. The ADCP measurements and numerical model simulations demonstrated a circulation of cold waters exiting Kvarner Bay in the southern part of the entrance, whereas during a Bora event, the outflow occurred in the northern part.

Keywords: ADCP, Bora wind, Istrian front, North Adriatic, Operational oceanography, Glider.

Introduction

Fronts

Fronts are an integral part of oceanic dynamics and play important roles in energy transfers from large-scale oceanic circulations of thousands of kilometres to small-scale phenomena limited to some metres. Fronts are the natural boundaries between water masses with different properties, but due to the diversity of their physical nature and to the different spatial and time scales, it is almost impossible to establish a clear definition (Ginzburg & Kostianoy, 2009). The most adopted definition was given by K. Fedorov, who determined that a frontal zone is a zone in which the 'spatial gradients of the main thermodynamic characteristics are very high in comparison with the average' (Fedorov, 1986; Kostianoy & Nihoul, 2009).

Fronts can be detected in temperature, salinity or density (referred to as thermal, saline or density fronts, respectively). When the spatial gradients of temperate coincide with the gradients of salinity, we have a thermohaline front. In the Mediterranean, fronts can be found in many regions. In the Aegean Sea, offshore the eastern part of Limnos Island, an intense thermohaline front is formed between the Black Sea outflow from the Dardanelles and the Levantine Intermediate Water (LIW), which is advected from the south (Zervakis *et al*., 2004; Androulidakis & Kourafalou, 2011; Vervatis *et al*., 2011; Kokkini *et al*., 2014). In the eastern Alboran Sea, the Almeria – Oran convergent density front is controlled by the size and position of the Eastern Alboran Sea gyre (Tintoré *et al*., 1988). In the Balearic Sea, there are two main frontal structures. The first is the Catalan density front in the centre of the Balearic subbasin, which separates old Atlantic Water (AW) from the less dense water transported by the Northern Current, and the second is the saline shelf/slope Balearic front, which separates the old AW from the fresher water transported by the Balearic Current (Wang *et al*., 1988; La Violette *et al*., 1990; Ruiz *et al*., 2009). A strong thermal front is located in the western Gulf of Lions and is associated with local upwelling (Millot, 1979; Nencioli *et al*., 2016).

In the Adriatic Sea, there are two predominant fronts—that generated by the Po River discharge in the northeastern Adriatic and the thermohaline IF off the northern Croatian coast. The dynamics of the latter are presented in this paper.

Study Area

The Adriatic Sea is a continental basin and represents the northernmost part of the Mediterranean Sea. It is located between the Italian Peninsula and the Balkans and is enclosed between two mountain chains, the Apennines and the Dinaric Alps. It is elongated, oriented SE to NW and has a length of 800 km and a mean width of 180 km (Fig. 1a). The Adriatic is connected to the Ionian Sea through the Strait of Otranto, which is only 74 km wide (Russo & Artegiani, 1996). Geomorphological characteristics of the Adriatic Sea play an important role in controlling its circulation dynamics. The study area, the northern Adriatic (NA), is a shallow coastal area with an average depth of 50 m.

Due to its position, the NA is subject to highly variable atmospheric forcing. The southeasterly Sirocco and northeasterly Bora winds are the predominant winds in the area (Poulain *et al*., 2003). As a result, the oceanographic properties of the NA, including the circulation and distribution of its water masses, strongly depend on the characteristics of air-sea fluxes (Cushman-Roisin *et al*., 2001). During winter in particular, the NA experiences events of intense and cold Bora winds. The Bora is a katabatic and gusty northeasterly wind that blows in the offshore direction on the eastern Adriatic coast (Zore-Armanda & Gačić, 1987). It is considered the strongest wind in the area. The frequency and intensity of this strong jet-like wind, which is characterized by strong horizontal shear, influence the whole structure of the water column and the NA circulation (Boldrin *et al*., 2009). Horizontal variations in the Bora wind cause variable oceanic cyclonic and anticyclonic patterns that drive the coastal waters into the middle of the basin (Orlić *et al*., 1992).

The general surface circulation of the NA (Fig. 1a) may be described as a large-scale cyclonic meander that includes *i)* the East Adriatic Current (EAC), which is a weak northwestward current located to the east that brings the Levantine Intermediate water (LIW) along with the Ionian surface water into the Adriatic Sea, and *ii)* the stronger and faster Western Adriatic Current (WAC) to the west, which is strongly influenced by the Po River discharge (Orlić *et al*., 1992; Poulain, 2001; Ursella *et al*., 2007). The Po River is the largest Italian river; the mean discharge is 1465 m^3s^{-1} and is highly variable (with a standard deviation of approximately 1056 m^3s^{-1}). The main peaks are recorded in May (due to snow melting) and in October–November (due to high precipitation) (Tedesco *et al*., 2007). The Po River plume is strengthened by the presence of low salinity water along the northern coast and is characterized by a strong cyclonic flow. This opposes the tendency for northward expansion of the Po River plume along the NA, and the predominant flow of Po waters is therefore southward (Kourafalou, 1999).

During winter, the NA circulation is primarily driven by lateral thermohaline variations in the fresher and colder water on the western side and the warmer and saltier water on the eastern side (Hendershott & Rizzoli, 1976; Artegiani *et al*., 1997) and secondarily modified by wind forcing (Hopkins *et al*., 1999). In particular, the persistent Bora wind can form two gyres, one in the northernmost part that is cyclonic and a second just to the south of the previous one that is anticyclonic (Zore-Armanda & Gačić, 1987; Orlić *et al*., 1994; Mauri & Poulain, 2001). A weak anticyclonic circulation feature is also located off Istria and between the strong cyclone to the north and the EAC recirculation branch to the south (Zore-Armanda, 1956; Poulain *et al*., 2001; Ursella *et al*., 2007).

During winter, atmospheric forcing can strongly affect the density structures in the relatively shallow NA. An intense Bora wind produces strong surface cooling and intense evaporation, thus making the water denser (Poulain *et al*., 2001; Lee *et al*., 2005a, b; Janeković *et al*., 2014; Vilibić *et al*., 2016). The resulting dense waters tend to spread out over the whole basin, moving to the southern region (Carniel *et al*., 2012; Vilibić & Supić, 2005). Density gradients, which are induced by the buoyancy flux and the coastal freshwater input, create fronts and are capable of driving a cyclonic flow in the Adriatic (Orlić *et al*., 1992).

In the NA, the early use of Advanced Very High Resolution Radiometer (AVHRR) images in the early 1980s by Phillippe & Harang (1982) showed a persistent front crossing the NA south and southwest of the Istria Peninsula (the peninsula between the Gulf of Trieste and Kvarner Bay) that separated the colder and less saline water of the northernmost part of the NA from the warmer and more saline water of southern origin. We refer to this front as the Istrian Front (IF). The existence of such a front has also been reported during surveys in the NA (Zore-Armanda, 1983; Lee *et al*., 2005a, b; Poulain *et al*., 2003). Model simulations have also been used to examine the thermohaline circulation in the NA and the persistence of the front under different wind conditions (Kuzmić *et al*., 2006; Vilibić *et al*., 2008; McKiver *et al*., 2016).

The multiplatform North Adriatic Experiment (NAE) occurred on the eastern coast of the NA from December 2014 to August 2015. During the targeted observation period in February 2015, one glider, one towed vehicle, one profiling float and several drifters were deployed, in addition to three long-term operating ADCPs. In this paper, the spatial structure of the IF and its response to wind changes are described. The high-resolution glider data are compared with the ADCP measurements to assess the spatio-temporal variability of the IF and the circulation at the entrance of Kvarner Bay during the NAE in the winter of 2015. Finally, the results are compared with those of previous experiments and existing numerical models.

Materials and Methods

Glider Data

Gliders are autonomous underwater vehicles that are equipped with oceanographic sensors. They move through the ocean following a saw-tooth pattern between the surface and a prescribed depth by changing their buoyancy. They can achieve vertical speeds of 10 – 20 cm s^{-1} and can move through the ocean with a forward speed of approximately 30 – 40 cm s^{-1} while performing dives and ascents at angles of approximately 26°. When underwater, they use a simple dead reckoning algorithm (based on computed speed and heading) to estimate their location until the next periodic surfacing. At the surface, they connect to an Iridium satellite to transmit the data and, most importantly, to get a precise GPS location. Any difference between the GPS fix and the final dead reckoning position is due to water currents while the gliders are moving underwater. This allows estimations of depth-averaged currents during glider missions (Stommel, 1989; Merchelbach *et al*., 2008; Rudnick *et al*., 2012).

During the NAE, the shallow (200 m) Slocum glider 'Leonardo' was used. This glider is designed to operate in coastal areas in depths of 4 to a maximum 200 m. 'Leonardo' was deployed in front of Kvarner Bay at 44.77° N and 13.69° E (point A in Fig. 1b) on 24 February 2015 at 10:00 GMT. It followed an almost straight trajectory southeastward until it reached 44.54° N and 13.99° E (point B in Fig. 1b) and turned back. It was recovered on 27 February 2015 at 09:00 GMT at 44.66° N and 13.85° E (point C in Fig. 1b). During the mission, the glider performed approximately 540 'yos' (equivalent to 1080 CTD casts) and 90 surfacings, which yielded a very high-resolution dataset. The maximum depths of the performed 'yos' varied from 20 to 45 m.

The glider was equipped with *i*) a Sea-Bird GPCTD sensor, which measures water temperature, pressure and salinity (derived by conductivity), *ii*) an Aanderaa Optode 4831 oxygen sensor to measure oxygen concentration and *iii*) a WetLab ECO Triplet FLBBCD-SLK sensor that provides data on chlorophyll fluorescence at 470/695 nm, back-scattering at 700 nm and Coloured Dissolved Organic Matter (CDOM) concentrations at 370/460 nm.

The glider provided a continuous dataset that covered a 55 km horizontal distance and was composed of two parts: the part from points A to B (~35 km), when the glider headed southeastward, and the repeated second part from points B to C (~20 km), when the glider headed northwestward to the recovery position.

Due to the high resolution of the measurements (measurements were taken at almost every 10 cm in depth and 5 seconds in time), no interpolations were applied to the original data. Only the longitudes and latitudes were linearly interpolated in time because the glider only provided exact positions during the surfacings. A simple, first step quality control was applied to all the data to remove outliers (spikes). For better visualization, the data were projected to an idealized path and plotted versus the distance of the initial point of deployment.

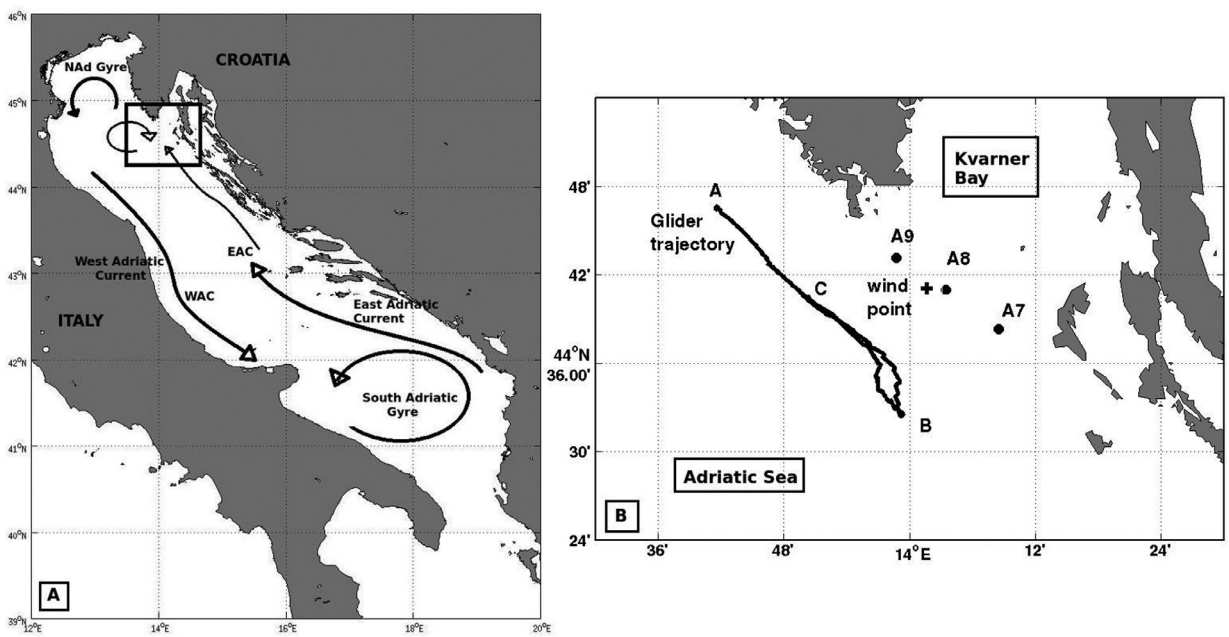

Fig. 1: A) Circulation features of the study area. B) Representation of the glider trajectory and ADCP positions. The black line indicates the glider trajectory between 24 and 27 February 2015, starting from point A, going to point B, turning back, and ending at point C. The ADCP stations A7, A8 and A9 are also depicted. The cross indicates the grid point where the ALADIN/HR wind data was extracted.

ADCP Data

Acoustic Doppler Current Profiler (ADCP) data from three stations in front of Kvarner Bay were collected during the NAE. The three Teledyne – RDI ADCPs were deployed at 44.64° N and 14.14° E, 44.68° N and 14.05° E and 44.72° N and 13.98° E, and those positions henceforth will be referred to as A7, A8 and A9, respectively. The deployment depths for A7 and A8 were 48 m, their working frequencies were 300 kHz, and A9 was deployed at 46 m and had a working frequency of 600 kHz. The sampling intervals were 10 minutes, and the averaging bin size was 2 m. Seabird SBE 16+V2 recorders were mounted on A7 and A9, and an SBE 26+ was mounted on A8; the recorders captured the bottom water temperature and salinity measurements.

Ancillary Data and models

Three-hourly data on surface wind components were extracted from the operational ALADIN/HR wind model (Tudor *et al*., 2013), which provides winds at 2 km spatial resolution via a dynamical adaptation technique every 3 hours. The grid point at the entrance of Kvarner Bay was chosen to represent the wind over the area (see Fig. 1b).

The use of a glider was insufficient to cover the spatial variability of the IF, and complementary data were therefore needed. For that reason, the results from a local coupled high-resolution atmosphere-ocean modelling system were used. The Regional Ocean Modelling System (ROMS) has a 2 km resolution, and its lateral boundary conditions were obtained from the operational AREG Adriatic model. The model's atmospheric forcing was also obtained from ALADIN/HR, whereas the other bulk variables were computed at 8 km resolution and used every 3 hours (Janeković *et al.*, 2014).

Satellite data of Sea Surface Temperature (SST) and ocean colour (chlorophyll concentration), from the moderate-resolution imaging spectroradiometer (MODIS-Aqua) were downloaded and processed at OGS. Due to high cloudiness, useful images were obtained only on 20 and 27 February 2015.

Results

Wind forcing

The glider deployment began under a weak easterly wind (~100° and ~5 m/s; see Fig. 2a). Conditions then changed to an ENE Bora (~55°) with increasing intensity (with a maximum of 15 m/s). The area remained under the Bora's influence until noon GMT on 26 February 2015, when the winds changed to weak easterly (~90° and ~5 m/s). When the glider crossed the IF for the first time, the strong Bora had already been blowing in the region for almost a day, and the second crossing occurred under the weakened easterly wind. These two different situations will be presented in detail below.

The Istrian Front

As the glider began its first southeastward trajectory, it measured a homogeneous water mass with an average temperature of approximately 10.6 °C and a salinity of ~ 37.6. It then encountered the sharp IF at 44.6° N latitude (the first front crossing is depicted in Fig. 3a by the letter P), which was almost vertically homogeneous down to the bottom. The front width was approximately 2.4 km, and the sea surface temperature (SST) gradient across it was ~0.55 °C/km, whereas the salinity and density gradient were 0.27 km^{-1} and 0.15 kg/m^3/km, respectively. After crossing the front, the glider measured the advected (from the south) waters, which had an average temperature 12 °C and an average salinity of 38.4, until it reached point B, where it turned back and started a northward trajectory. At latitude 44.53° N and under a weaker wind, the glider crossed the IF for the second time. The front, which was smoother and inclined, was characterized by the presence of a transitional water mass that was elongated over some kilometres. The width of the IF was approximately 8 km, and the SST gradient across it was ~0.16 °C/km (0.08 / km for salinity and 0.04 kg/m^3/km for the density gradient) (Fig. 3c, d). All the horizontal surface gradients of temperature, salinity and density for both front crossings are listed in Table 1. The mission continued, and the glider again measured the homogeneous well-mixed and cold NA water, until it reached point C, where it finished its mission and was recovered.

The density followed the salinity profile well (Fig. 3b). In the first transect, the sigma-theta was estimated approximately 28.8 kg/m^3 in the surface layers and approximately 28.9 kg/m^3 in the deeper layers. The frontal zone was present in the density profile and depicted a sharp and vertical IF. South of the front, the sigma-theta was 29.23 kg/m^3. During the second frontal crossing, the density front was smoother and more inclined than in the salinity front, but it was still present.

In addition to physical parameters, the glider also measured oxygen concentration. At the beginning of the experiment, the oxygen concentrations were higher (~ 6.2 ml/l) than during the remainder of the mission. Heading southeastward, the concentrations decreased gradually to 5.8 ml/l until reaching the frontal zone, where the oxygen concentrations were measured at less than 5.6 ml/l (Fig. 3e). During the northwestward transect, the oxygen concentrations on the wide and relaxed front were ~ 5.7 ml/l. Thus, the IF was also clearly manifested in the oxygen data.

The chlorophyll measurements are presented in Figure 3f. The glider initially encountered waters with very low chlorophyll concentrations (0.2 mg/m^3). South of the front, higher chlorophyll concentrations were measured, the average value of which was 0.7 mg/m^3. Filaments of

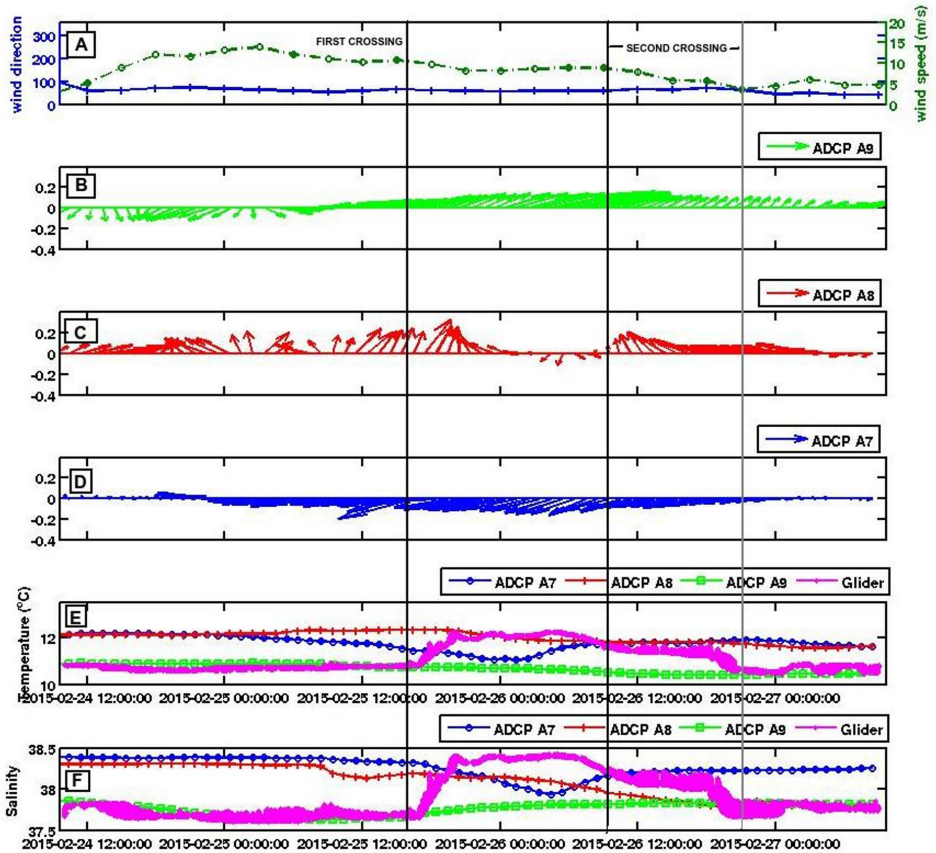

Fig. 2: A) Wind from ALADIN/HR model, B) ADCP A9 station, depth-averaged current measurements, C) ADCP A8 station, depth-averaged current measurements, D) ADCP A7 station, depth-averaged current measurements, E) Temperature plot of the ADCPs stations bottom measurements and the glider data, F) Salinity plot of the ADCPs stations bottom measurements and the glider data. The black vertical lines are depicting the two times when the glider was crossing the IF. The gray line refers to the time that the glider finished the second crossing. Hours are GMT.

negligible chlorophyll were found in front of Kvarner Bay, and they were also present in the satellite images in that area (as depicted in Fig. 4).

With measured values that varied from 0 to 1.5, the CDOM (not shown) was considered to be significantly low during the entire glider mission and was near the optical sensor's resolution. The CDOM profiles were inversely related to the salinity (and chlorophyll) profiles, as is generally the case in coastal areas.

The backscatter data (not shown) followed the salinity profile very well, in contrast to CDOM. The northern part was reported as a region with decreased backscatter, whereas south of the front, the backscatter increased. A region of decreased backscatter was measured during the northwestward trajectory, which corresponded to the low salinity filaments in that area.

The spatio-temporal variability of the Istrian Front

Satellite images of SST and chlorophyll concentration were also used to determine the IF position. The satellite images confirmed that the front was in an approximately zonal direction extending westward from the entrance to Kvarner Bay and that the Po River discharge was limited to the northern part of the NA and along the western Italian coast (Fig. 4).

As mentioned above, three ADCPs were deployed at the entrance of Kvarner Bay. Fig. **2**b,c,d show the hourly depth-averaged currents measured at stations A9, A8 and A7, respectively, the temperature and salinity of the bottom waters, and the temperature and salinity measured by the glider (Fig. 2e,f). Station A9 was always under the influence of the NA cold and less saline waters, whereas A8 measured constantly warmer waters, but its salinity followed a decreasing trend. In contrast, the southernmost station, A7, seemed to be significantly influenced by the local wind conditions. Initially, A7 registered a weak northwestward current and a bottom temperature and salinity similar to those measured at A8. When the wind changed to a strong Bora, the measured current acquired a strong southwestward direction, the bottom temperature decreased by more than 1 °C, passing from above 12 °C to almost 11 °C, and the salinity decreased by 0.5 from 38.5 to almost 38.

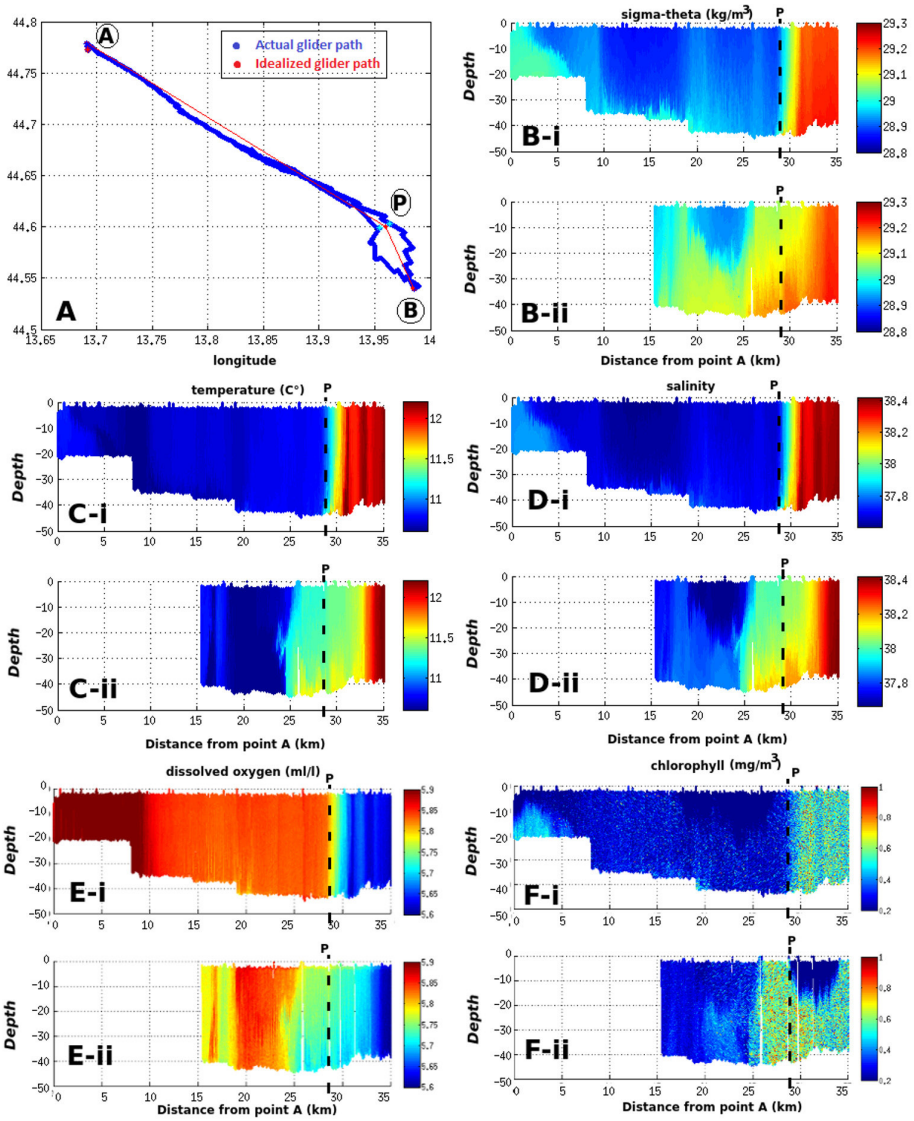

Fig. 3: Plots of the two glider transects, versus distance from the starting point A. The glider data are projected to the idealized path, as it is shown in panel A and the letter P is depicting the position of the IF during the first crossing. The upper panels (-i) are showing the rout from point A to point B and the lower panels (-ii) are showing the rout from point B back to point A, for B) sigma-theta, C) temperature, D) salinity, E) dissolved oxygen and F) chlorophyll concentration.

Afterwards, as the wind calmed, the A7 temperatures returned to their initial values.

The glider measurements showed a mainly homogeneous water column north and south of the front. Thus, a comparison of the bottom temperature measured by the glider with the bottom temperature measured by the ADCPs can provide an estimate of the spatio-temporal variability of the frontal features during the experiment. Six snapshots of hourly averaged glider and ADCP temperature measurements were chosen for comparison (Fig. 5). In addition, all the maps depict the hourly depth-averaged current measured by the ADCPs and the glider.

At the time of the Bora maximum (Fig. **5**a), the glider and A9 were measuring north Adriatic waters (<11 °C). The glider was measuring a weak southward current, whereas A9 showed a weak eastward current heading into Kvarner Bay. A8 and A7 showed temperatures near 12.8 and 12.5 °C, respectively. A strong (~15 cm/s) southwestward current was measured at A7. Afterwards, (Fig. 5b), the glider moved to the south and encountered warmer waters (>11.5 °C). The temperature at A8 was ~13 °C, whereas at A7, the temperature decreased (~12 °C). A very strong westward current was present at A7 (Fig. **5**b), which then appeared at A7 and at the glider position (Fig. 5c). The current changed to a southwest direction and maintained its high speed, whereas the temperature decreased. This strong current was measured at the ADCP stations and by the glider (Fig. 5c, d). The glider then started its northwestward trajectory (Fig. 5e) under a weaker wind forcing and measured waters with temperatures of ~11.8 °C,

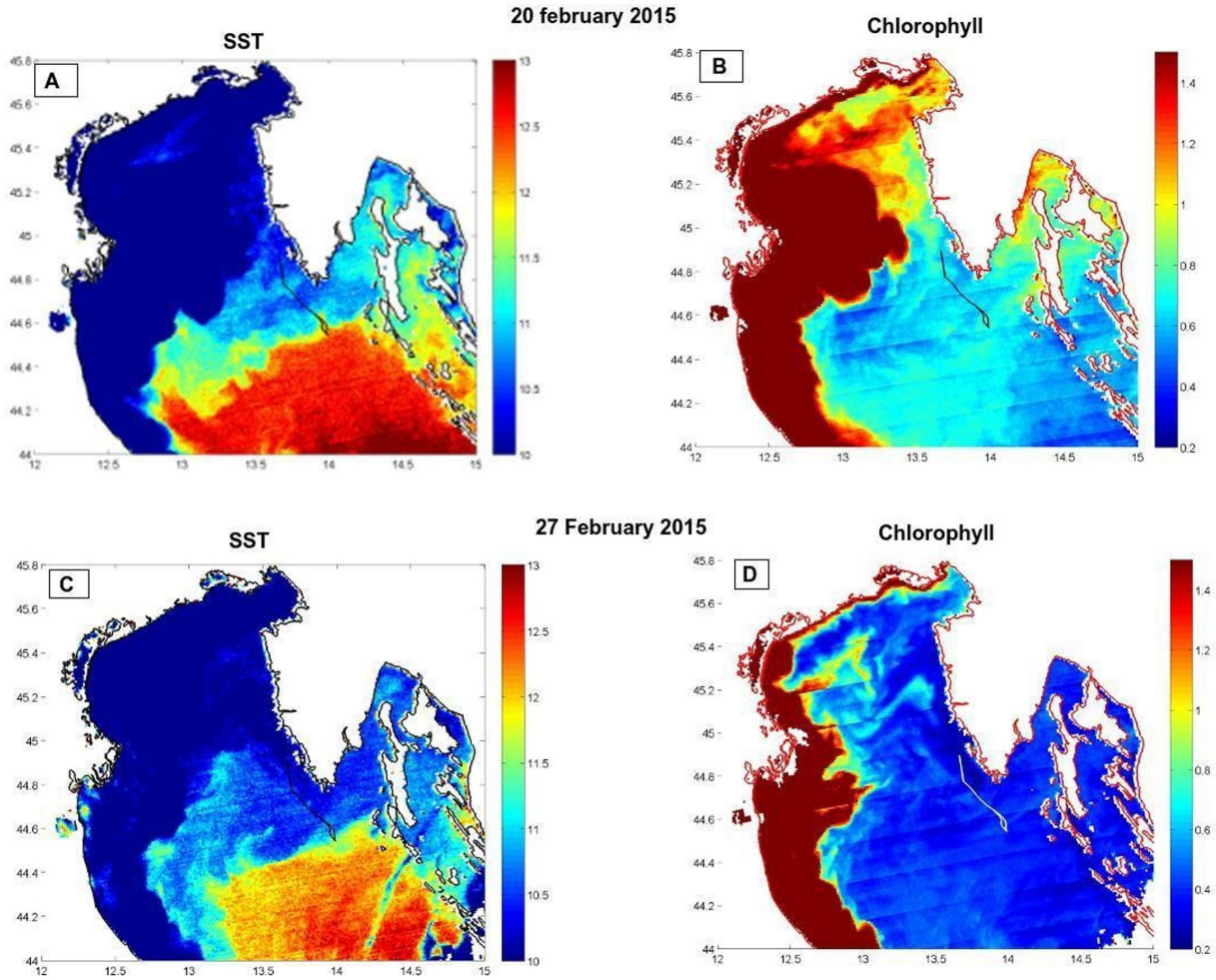

Fig. 4: Satellite images from MODIS. A) and B) are depicting the SST and the chlorophyll respectively, measured in 20 February 2015, while C) and D) show the same for 27 February 2015.

whereas at the entrance to Kvarner Bay, the temperatures were higher (~12.4 °C at A8 and A7). At the end, the glider re-entered north Adriatic waters (Fig. **5**f) and finished its mission. Station A9 remained under the influence of the north Adriatic cold waters during the entire glider mission, whereas the other ADCP stations demonstrated the dynamic variability of the Istrian frontal features and a water mass circulation outward of Kvarner Bay under a strong Bora event, with a counter flow closer to the Istrian coast.

The results of the 2 km resolution, whole-Adriatic ROMS model were also used with the field measurements. The model showed a homogeneous water column with some small differences with depth in the current velocities and circulation pattern inside Kvarner Bay. We selected some snapshots of the model simulations (for the surface layer only) during the glider operation (Fig. 6). The model results evidenced the dynamics of the Istrian Front and the main response of the shallow Kvarner waters to the wind. In particular, they confirmed that the cold measured waters at ADCP station A7 originated inside Kvarner Bay.

Discussion

The glider crossed the IF twice; in the first crossing, the strong Bora wind was blowing, and in the second crossing, the wind had weakened and slightly changed direction. During the first crossing, the IF was sharp, almost vertical and extended down to the bottom, and the surface temperature changed 1.2 °C within a distance of 2.4 km. During its second crossing, the IF started to be inclined and relaxed and was weaker and much wider (the changes in temperature, salinity and density occurred over a distance of 8 km). If we consider that the two different conditions were observed less than a day apart, the IF was characterized by its fast reaction to the wind forcing.

A density front coincident with this thermohaline Istrian front was also observed, in contrast to previous studies in which the IF was approximately compensated in density (Zore-Armanda & Gačić, 1987; Poulain *et al*., 2003, 2011). Indeed, during a previous experiment that was carried out in the same area in 2003 (DOLCEVITA experiment, Poulain *et al*., 2003), a very strong temperature gradient

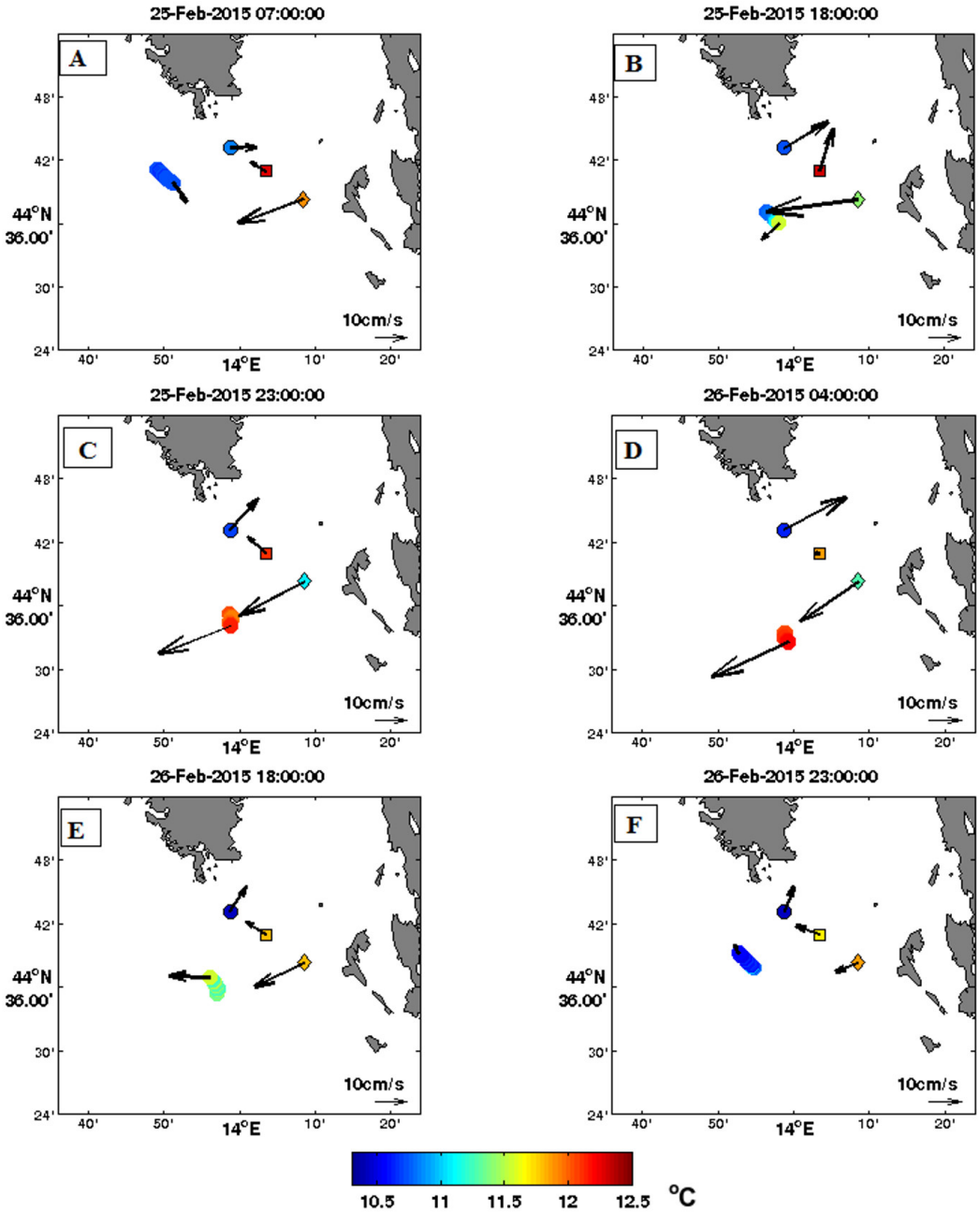

Fig. 5: Selected hourly snapshots of the study area during the glider position and the ADCP hourly and depth-averaged currents (arrows).

Table 1. Horizontal gradients (per km) of the main physical parameters (temperature, salinity and density) for the first and the second IF crossings.

	Temperature (°C/km)	Salinity (km^{-1})	Density ($kg/m^3/km$)
First crossing	0.55	0.27	0.15
Second crossing	0.16	0.08	0.04

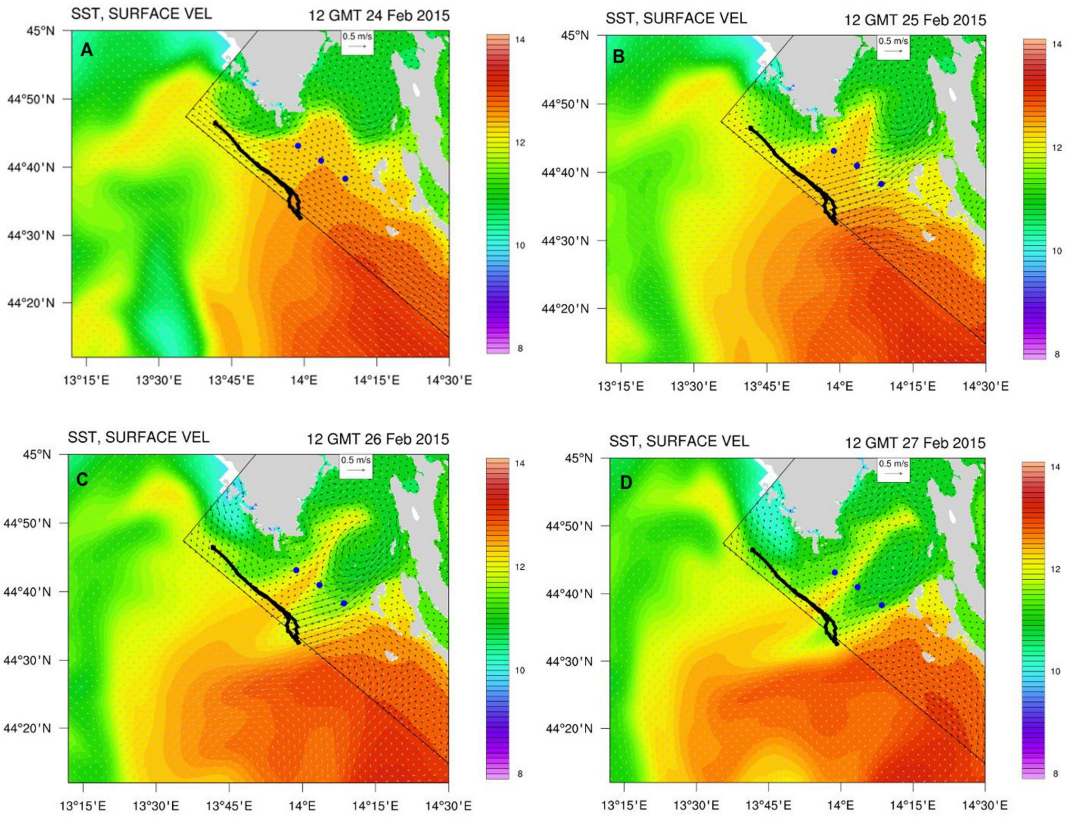

Fig. 6: Selected snapshots of the ROMS model (surface currents – black arrows and color coded SST) contemporaneous to the glider operation.

(~3 °C/km) at the IF was approximately compensated by salinity, resulting in a negligible density gradient (Poulain *et al*., 2011). In contrast, in February 2015, the glider measured a density difference of ~0.25 kg/m^3/km during the first front crossing and a relaxed density front with a difference of 0.04 kg/m^3/km during the second crossing.

The IF was evident in the dissolved oxygen data, with the area north of the IF depicting slightly higher values of dissolved oxygen than those in the southern area. We can easily distinguish an inverted correlation between salinity/temperature and dissolved oxygen. This is consistent with the dependence of oxygen concentration on hydrological parameters because oxygen solubility in seawater is inversely correlated with temperature and salinity (Green & Carrit 1967; Tromans, 1998).

The satellite images of chlorophyll distribution (Fig. 4b, d) show that the Po discharge was limited to the western part of the NA. They also depict a high chlorophyll concentration inside Kvarner Bay, when the area was under the Bora wind (Fig. 4b). Considering the circulation at the entrance of Kvarner bay (the outward direction in the southern part of the entrance), we speculate that the presence of higher chlorophyll concentrations south of the front originate inside Kvarner Bay.

Zore–Armanda & Gačić (1987), referring to the importance of the IF, reported that water masses were sinking in that area, probably due to the convergence at the IF. Through that mixing process, waters of higher salinity and lower temperature are formed, which could make the Istrian front a preferable site for dense water formation during the winter season in the NA (Zore-Armanda & Gačić, 1987). The preconditioning of the dense water formation in the NA in dry years with reduced freshwater river outflows results in increased salinity in combination with extended periods of cold and severe winds, which cause heat loss (Mihanović *et al*., 2013; Janeković *et al*., 2014; Vilibić *et al*., 2016). However, in the winter of 2015, the situation was somewhat different. Bora events were present before and during the study period, but they were characterized by very short durations—probably too short for triggering dense water formation. Furthermore, the preceding November and December months were exceptionally wet.

The high-resolution glider data also provided an opportunity to observe a small thermohaline intrusion during the northward crossing of the IF. The small thermohaline intrusion was observed in temperature and salinity (and in the oxygen data). It was located at a depth of 15 m, extended to 35 m vertically and was horizontally elongated

from the smooth and weak side of the Istrian front for approximately 1.5 km. The occurrence of these 'abnormal' temperature or salinity variations within the water column can depict lateral flows. Those flows, which occur on both sides of the front and transport water masses from one side to the other, can contribute to the lateral exchange process across the front (Li & Wang, 2013).

Conclusions

In this work, the use of a Slocum glider gave us an opportunity to observe the IF at high resolutions and to study its responses to a rapid change in winds. This well-defined front was also observed in satellite images of SST and was found to be zonally orientated, extending westward from outside Kvarner Bay and reaching the Italian coast. The area southwest of the Istrian Peninsula, which is the area where the IF is located, is a very dynamic area that is strongly influenced by local wind conditions. The available of in situ data (glider and ADCP data), satellite images and available Adriatic model outputs revealed a very dynamic response of the Kvarner Bay waters to the wind changes, especially under the influence of a Bora event. The cold waters from inside the bay were found to flow out in the southern part of the entrance, whereas in the northern part, closer to the Istrian coast, warmer waters were advected into the bay. This was an unexpected behaviour because, under Bora wind forcing, a strong outflow is usually present in the northern part of the entrance of Kvarner Bay, and an inflow is present in the southern entrance (Book *et al*., 2007). The model results for the circulation clearly reproduced the ADCP measurements very well.

In conclusion, this observational experiment (NAE) has demonstrated the usefulness of employing a glider to monitor the spatial variability of coastal areas in an operational mode. In this study area, the shallow Slocum glider was appropriate because the vertical extension of the IF reaches to the bottom of the NA, which is only approximately 50 m in depth. The glider was able to monitor the area, even under adverse meteorological conditions. This fact is of great importance because traditional sampling methods such as the use of research vessel CTDs or towed vehicles must usually be cancelled under the same conditions. Thus, the ability of longer glider deployments operating under different meteorological conditions and alongside ADCP measurements could provide data to better understand the response of the IF to various wind conditions. These data could also be assimilated into local numerical models.

Acknowledgements

A part of this work has been supported by the Croatian Science Foundation under contract IP-2013-11-5928 (project ADAM-ADRIA). The authors would like to thank Piero Zuppelli, Stefano Kuchler and Antonio Bussani for their precious help during the glider operations and data processing. Finally, we would like to thank the unknown reviewers who helped us improve this work.

References

Androulidakis, Y.S., Kourafalou, V.H., 2011. Evolution of a buoyant outflow in the presence of complex topography: the Dardanelles plume (North Aegean Sea). *Journal of Geophysical Research*, 116, C04019.

Artegiani, A., Bregant, D., Paschini, E., Pinardi, N., Raichich, F. *et al.*, 1997. The Adriatic Sea general circulation. Part I: Air-sea interactions and water mass structure, *Journal of Physical Oceanography*, 27, 1492-1514.

Boldrin, A., Carniel, S., Giani, M., Marini, M., Bernardi Aubry, F. *et al.*, 2009. Effects of bora wind on physical and biogeochemical properties of stratified waters in the northern Adriatic. *Journal of Geophysical Research,* 114, C08S92.

Book, J. W., Signell, R. P., Perkins, H., 2007. Measurements of storm and nonstorm circulation in the northern Adriatic: October 2002 through April 2003. *Journal of Geophysical Research*, 112, C11S92.

Carniel S., Bergamasco, A., Book, J. W., Hobbs, R. W., Sclavo, M. *et al.,* 2012. Tracking bottom waters in the Southern Adriatic Sea applying seismic oceanography techniques. *Continental Self Research*, 44, 40-48.

Cushman-Roisin, B., Gačić, M., Poulain, P.-M., Artegiani, A., 2001. Toward the future. p. 241-245. In: *Physical Oceanography of the Adriatic Sea*. *Past, Present and Future*. Cushman-Roisin, B., Gačić, M., Poulain, P.-M., Artegiani, A. (Eds.), Kluwer Academic Publishers, Dordrecht, The Netherlands.

Fedorov, K.N., 1986. *Physical Nature and Structure of Oceanic Fronts*. Vol. 9, Springer, New York, 333 pp.

Ginzburg A, Kostianoy A., 2009. Fronts and mixing processes. p. 237-268. In: Oceanography, Encyclopaedia of life support systems (EOLSS), Vol. 1. Chen, C. A., Nihou, J. C. J. (Eds.), UNESCO/EOLSS Publishers, Oxford.

Green, E.J., Carrit, D.E., 1967. Oxygen solubility in seawater: Thermodynamic influence of sea salt. *Science,* 157, 191-193.

Hendershott, M. C., Rizzoli, P., 1976. The winter circulation of the Adriatic Sea. *Deep-Sea Research*, 23, 353-370.

Hopkins, T.S., Kinder, C., Artegiani, A., Pariante, R., 1999. A discussion of the northern Adriatic circulation and flushing as determined from the ELNA hydrography. p. 85-106. In: *The Adriatic Sea. Ecosystem Report*. Hopkins, T. S., Artegiani, A., Cauwet, G., Degobbis, D., Malej, A., (Eds), European Commission, Brussels, Belgium, EUR 18834.

Janeković, I., Mihanović, H., Vilibić, I., Tudor, M., 2014. Extreme cooling and dense water formation estimates in open and coastal regions of the Adriatic Sea during the winter of 2012. *Journal of Geophysical Research*, 119, 3200-3218.

Kokkini, Z, Potiris, M, Kalampokis, A, Zervakis, V., 2014. Hf radar observations of the Dardanelles outflow current in the north eastern Aegean using validated WERA HF radar data. *Mediterranean Marine Science,* 15 (4), 753-768.

Kostianoy, A.J., Nihoul, J.C.J., 2009. Frontal Zones in the Norwegian, Greenland, Barents and Bering Seas p. 171-190. In: *Influence of Climate Change on the Changing Arctic and Sub-Arctic Conditions*. Nihoul, J., Kostianoy, A.J. (Eds), Springer Publishing Company, Dordrecht, The Netherlands.

Kourafalou, V., 1999. Process studies on the Po River plume, North Adriatic Sea. *Journal of Geophysical Research*, 104, 29963-29985.

Kuzmić, M., Janeković, I., Book, J.W., Martin, P.J., Doyle, J.D., 2006. Modeling the northern Adriatic double-gyre response to intense bora wind: a revisit. *Journal of Geophysical research,* 111, C03S13.

La Violette, P. E., J. Tintorè, and J. Font, 1990. The surface circulation of the Balearic Sea, *Journal of Geophysical Research,* 95, 1559-1568.

Lee, C., Askari, F., Book, J., Carniel, S., Cushman-Roisin, B. *et al.*, 2005a. Northern Adriatic response to a wintertime Bora wind event. *EOS*, 86 (16), 157-165.

Lee, C., Gobat, J., Jones, B., Poulain, P.M., Peters, H. *et al.*, 2005b. *Cruise Report: DOLCE VITA 1 and 2, 31 January - 24 February and 26 May - 15 June 2003*. Applied Physics Laboratory, University of Washington, Seattle, WA Technical Report, 315 pp.

Li, Y., Wang, F., 2013. Thermohaline intrusions in the thermocline of the western tropical Pacific Ocean, *Acta Oceanologica Sinica*, 32 (7), 47-56.

Mauri, E., P.M. Poulain, 2001. Northern Adriatic Sea surface circulation and temperature/pigment fields in September and October 1997. *Journal of Marine Systems*, 29, 51-67.

McKiver, W., Sannino, G., Bellafiore, D., 2016. Investigation of model capability in capturing vertical coastal processes: A case study in the Adriatic Sea. *Ocean Science*, 12, 51-69.

Merchelbach, L.M., Briggs, R.D., Smeed, D.A., 2008. Current measurements from autonomous underwater gliders. p. 61-67. In: *Proceedings of the IEEE/OES/CMTC Ninth Working Conference on Current Measurement Technology*, 17-19 March, Charlston, SC, USA.

Mihanović, H., Vilibić, I., Carniel, S., Tudor, M., Russo, A. *et al.*, 2013. Exceptional dense water formation on the Adriatic shelf in the winter of 2013, *Ocean Science*, 9, 561-572.

Millot, C., 1979. Wind induced upwellings in the Gulf of Lions. *Oceanologica. Acta*, 2, 261-274.

Nencioli, F., Petrenko, A.A., Doglioli, A.M., 2016. Diagnosing cross- shelf transport along an ocean front: An observational case study in the Gulf of Lion, *Journal of Geophysical Research Oceans*, 121, 7218-7243.

Orlić, M., Gačić, M., La Violette, P.E., 1992. The currents and circulation of the Adriatic Sea. *Oceanologica Acta*, 15 (2), 109-124.

Orlić, M., Kuzmić, M., Pasarić, Z., 1994. Response of the Adriatic Sea to the bora and sirocco forcing. *Continental Self Research*, 14 (1), 91-116.

Poulain, P.M., 2001. Adriatic Sea surface circulation as derived from drifter data between 1990 and 1999, *Journal of Marine systems,* 29, 3-32.

Poulain, P.M., Kourafalou, V.H., Cushman-Roisin, B., 2001. Northern Adriatic Sea. p. 143-165. In: *The Physical Oceanography of the Adriatic Sea. Past, Present and Future*. Cushman-Roisin, B., Gačić, M., Poulain, P.-M., Artegiani, A. (Eds.), Kluwer Academic Publishers, Dordrecht, The Netherlands.

Poulain, P.M., Ursella, L., Mauri, E., Deponte D., 2003. *DOLCEVITA-1 Cruise 31 January – 24 February 2003*. Report of drifter-related activities, Rel. 08/2003/OGA/03, OGS, Trieste, Italy, 32 pp.

Poulain, P.M., Lee C., Mauri, E., Notarstefano, G., Ursella, L., 2011. Observations of currents and temperature-salinity-pigment fields in the northern Adriatic Sea in winter 2003. *Bollettino di Geofisica Teorica ed Applicata*, 52, 149-174.

Rudnick, D.L., Baltes, R., Crowley, M., Schofield, O., Lee, C.M. *et al.*, 2012. pp. 1-5. A national glider network for sustained observation of the coastal ocean. In: *Oceans*, 14-19 Oct. IEEE, Hampton Roads, VA, USA

Ruiz, S., Pascual, A., Garau, B., Faugere, Y., Alvarez, A. *et al.*, 2009. Mesoscale dynamics of the Balearic front integrating glider, ship and satellite data. *Journal of Marine Systems*, 78, S3- S16.

Russo, A., Artegiani, A., 1996. Adriatic Sea hydrography, (60) p.33-43. In: *The European anchovy and its environment*, Palomera, I., Rubies, P. (Eds.). Scientia Marina, *Barcelona*.

Stommel, H. 1989. The Slocum Mission. *Oceanography,* 2 (1), 22-25.

Tedesco, L., Socal, G., Bianchi, F., Acri, F., Veneri, D. *et al*., 2007. NW Adriatic Sea biogeochemical variability in the last 20 years (1986–2005), *Biogeosciences*, 4, 673–687.

Tintoré, J., La Violette, P.E., Bladé, I., Cruzado, A., 1988. A study of an intense density front in the eastern Alboran Sea: The Almeria-Oran front. *Journal of Physical Oceanography*, 18, 1384-1397.

Tromans, D., 1998. Temperature and pressure dependent solubility of oxygen in water: a thermodynamic analysis. *Hydrometallurgy,* 48 (3), 327-342.

Tudor, M., Ivatek-Šahdan, S., Stanešić, A., Horvath, K., Bajić, A., 2013. Forecasting weather in Croatia using ALADIN numerical weather prediction model, p. 59-88. In: *Climate Change and Regional/Local Responses*. Zhang, Y., Ray, P. (Eds.). InTech, Rijeka, Croatia.

Ursella, L., Poulain, P.M., Singell, P., 2007. Surface drifter circulation in the northern and middle Adriatic Sea: Response to wind regime and season, *Journal of Geophysical Research,* 112, 1-18.

Vervatis, V., Sofianos, S., Theocharis, A., 2011. Distribution of the thermohaline characteristics in the Aegean Sea related to water mass formation processes (2005–2006 winter surveys). *Journal of Geophysical Research*, 116, C09034, 1-16.

Vilibic, I., Supic, N., 2005. Dense water generation on a shelf: The case of the Adriatic Sea. *Ocean Dynamics*, 55, 403–415.

Vilibić, I., Beg Paklar, G., Žagar, N., Mihanović, H., Supić, N. *et al.*, 2008. Summer breakout of trapped bottom dense water from the northern Adriatic, *Journal of. Geophysical Research*, 113, S1102-1-S1102-19.

Vilibić, I., Mihanović, H., Janeković, I., Šepić, J., 2016. Modelling the formation of dense water in the northern Adriatic: Sensitivity studies, *Ocean Modelling*, 101, 17-29.

Wang, D.P., Vieira, M., Salat, J., Tintoré, J., La Violette, P.E., 1988. A shelf/slope filament off the northeast Spanish coast, *Journal of. Marine Research*, 46, 321-332.

Zervakis, V., Georgopoulos, D., Karageorgis, A.P., Theocharis, A., 2004. On the response of the Aegean Sea to climatic variability: a review. *International Journal of Climatology,* 24, 1845-1858

Zore-Armanda, M., 1956. On gradient currents in the Adriatic Sea, *Acta Adriatica, 8* (6), 1-38.

Zore-Armanda, M., 1983. Some physical characteristics of the Adriatic Sea, *Thalassia Jugoslavica,* 19, 433-450.

Zore-Armanda, M., Gačić, M., 1987. Effects of bora on the circulation in the North Adriatic. *Annals of Geophysics*, 5, 93-102.